SEBHA UNIVERSITY JOURNAL OF PURE & APPLIED SCIENCES VOL.23 NO. 1 2024
DOI: 10.51984/JOPAS.V23I1.2508

مجلة جامعة سبها للعلوم البحتة والتطبيقية
Sebha University Journal of Pure & Applied Sciences

Journal homepage: www.sebhau.edu.ly/journal/index.php/jopas

Increasing Oil Recovery by Gas Injection for Libyan Carbonate Sedimentary Field (LCSF) by using Eclipse Software

*Madi Abdullah Naser[1], Omar Ibrahim Azouza[2], Salem Abdulsalam Elteriki[3]

[1]Department of Chemical and Petroleum Engineering, School of Applied Sciences and Engineering, Academy for Postgraduate Studies, Janzour, Tripoli, Libya.
[2]Department of Industrial Engineering and Manufacturing, Faculty of Engineering, Misurata University, Misurata, Libya.
[3]Department of Industrial Engineering, College of Industrial Technology, Misurata, Libya.

Keywords:
Oil Recovery
Gas Injection
Libyan Carbonate Sedimentary
Eclipse Software

ABSTRACT

In this study, two software MBAL - Petroleum Experts and Eclipse are used to do comprehensive reservoir study for LCSF plane of development, this study covered analyses and evaluation. Gas injection essentially increases the rate of oil field development and in many cases permits increased oil recovery. This paper demonstrates a successful simulation case study based on a field data of a project. The objective of this study is to improve recovery from Libyan Carbonate Sedimentary Field by three wells of gas injection. To do that, first, the simulation 3-D model was built by using advanced reservoir simulation software (Schlumberger Eclipse). Second, select the best zone for gas injection. Third, select the best location for injector well. Fourth, determine the injector well depth. The results of the paper can be seen to match the real data of the reservoir with the results of the program using a MBAL software. The simulator results show the reservoir pressure history curve is matching to the stimulation curve, this gives a good allusion of the input data that has been entered to the model. The driving mechanism of this reservoirs it comes from three natural forces, which are fluid expansion, PV compressibility, and water influx. Gas injection scenario has a good plateau bpd lasts approximately 3 years and after that started to decrease. The Cumulative oil production is 108442340 STB barrels of oil with the recovery factor approximately 0.52805 and final reservoir pressure is maintained 328.76 pisa

زيادة استخلاص النفط عن طريق حقن الغاز لحقل الكربونات الرسوبي الليبي (LCSF) باستخدام برنامج Eclipse.

*مادي عبدالله نصر[1] و عمر إبراهيم اعزوزة[2] و سالم عبد السلام التريكي [3]

[1]قسم الهندسة الكيميائية والنفط، مدرسة العلوم التطبيقية والهندسية، الاكاديمية الليبية للدراسات العليا، جنزور طرابلس، ليبيا.
[2]قسم الهندسة الصناعية والتصنيع، كلية الهندسة، جامعة مصراته، مصراته،ليبيا.
[3]قسم الهندسة الصناعية، كلية التقنية الصناعية،مصراته،ليبيا.

الكلمات المفتاحية:
استخلاص النفط
حقن الغاز
برنامج Eclipse
رواسب الكربونات الليبية

الملخص

في هذه الدراسة، تم استخدام برنامجين MBAL - Petroleum Experts وEclipse لإجراء دراسة شاملة للمكمن لخطة تطوير، وقد تم عمل في هذه الدراسة التحليلات والتقييم. يؤدي حقن الغاز بشكل أساسي إلى زيادة معدل تطوير حقول النفط ويسمح في كثير من الحالات بزيادة استخراج النفط. توضح هذه الورقة دراسة حالة محاكاة ناجحة تعتمد على البيانات الميدانية. الهدف من هذه الدراسة هو تحسين الاستخلاص من حقل الكربونات الرسوبي الليبي عن طريق حقن الغاز في ثلاث آبار. وللقيام بذلك، تم أولاً إنشاء نموذج المحاكاة ثلاثي الأبعاد باستخدام برنامج محاكاة المكامن المتقدم (Schlumberger Eclipse). ثانيا، تحديد أفضل منطقة لحقن الغاز. ثالثًا، تحديد أفضل موقع لبئر الحاقن. رابعاً، تحديد عمق بئر الحاقن. ويمكن النظر إلى نتائج الورقة مطابقة للبيانات الحقيقية للمكمن مع نتائج البرنامج باستخدام برنامج MBAL. تظهر نتائج المحاكاة

*Corresponding author:
E-mail addresses: madi.naser@academy.edu.ly, (O. I. Azouza) Omar.i.azouza@gmail.com, (S. A. Elteriki) salematriki@yahoo.com
Article History : Received 20 March 2023 - Received in revised form 23 October 2023 - Accepted 27 January 2024

أن منحنى تاريخ ضغط الخزان يتطابق مع منحنى المحاكاة، وهذا يعطي إشارة جيدة لبيانات الإدخال التي تم إدخالها إلى النموذج. يتكون الدفع الطبيعي للمكمن من ثلاث قوى طبيعية، وهي تمدد السوائل، وانضغاطية الحضور، وتدفق المياه. سيناريو حقن الغاز لديه ثبات جيد للإنتاج يستمر حوالي 3 سنوات وبعد ذلك بدأ بالانخفاض. يبلغ إنتاج النفط التراكمي 108442340 برميلًا من النفط مع عامل استرداد يبلغ حوالي 0.52805 وتم الحفاظ على ضغط الخزان النهائي عند 328.76 ضغط جوى.

Introduction

The oil recovery process is an essential element in the oil industry, Naser et al, 2018 [1]. There are many known enhanced oil recovery (EOR) methods, and every method has criteria for use. Some of those methods are gas injection, such as CO_2 injection, N_2 and hydrocarbon gas injection. CO_2 has been the largest contributor to global EOR, Samba, et al 2020 [2]. Gas injection is an enhanced oil recovery method. Inert gases, typically nitrogen or carbon dioxide, are pumped into an injection well. This creates higher pressure that filters through the reservoir formation and pushes hydrocarbons out from low pressure or isolated areas.

Cuiyu, et al, 2013 [3] used a numerical reservoir simulator to evaluate the performance of CO_2 injection for the Bakken interval in a sector of the Sanish Field. Several different scenarios of gas injection are tested to analyse gas injection performance and evaluate its technical feasibility and effect. It appears that gas injection is suitable in such tight environments, as the recovery factors increased significantly for miscible CO_2 injection.

Baojun, et al, 1997 [4], piloted test of water alternating gas injection in heterogeneous thick reservoir of positive rhythm sedimentation of Daqing Oil Field. The study showed that the recovery factor is now more than 3% higher than the ultimate recovery factor by water injection, and the ultimate recovery is predicted to be more than 8% higher. Areal sweep conditions are improved, and the thickness of liquid production increases. Another study conducted by Hedjazi and others in 1976, [5], showed that the areal sweep conditions are improved and the thickness of liquid production is increased. Reservoir calculations indicated that only 12.5% of the original oil in place could be recovered by normal depletion, but that recovery could be increased to 22.8% by gas injection, Hedjazi, et al 1976 [5]. The early initiation of pressure maintenance by gas injection and exercising close control of producing operations will yield an ultimate recovery of approximately 70.5 percent of the original oil in place [6]. Reservoir simulation indicated that the ultimate recovery factor is expected to be over 50% with such full-field gas injection, Tang, et al 2013 [7]. CO_2 flooding suitability for shale oil reservoirs with low permeability, low porosity, and rich organic matter (kerogen) remains controversial [8]. The simulation results show an approximately 7.5% increase in gas production and an approximately 8% increase in oil produced at a temperature of approximately 200 F, considerably higher than the 2.4% and 4% gas and oil produced at a lower injected temperature of 120 deg F, Ibe,, et al 2022 [9]. The gas injection project has increased the reservoir pressure from 500 psi to 700 psi, Ariffin, et al 2022 [10].

Numerical results indicated that injection schemes based on highly slanted wells and water alternating gas injection can overcome early gas breakthrough and a considerable amount of gas emissions, providing an improved sweep efficiency, a stable displacement and a significant degree of CO_2 retention, Rotelli,, et al 2017 [11]. The injected gas has a negligible opportunity cost owing to sales gas export constraints. This combination of factors yields a highly economic project, Jethwa, et al 2002 [12]. Nitrogen injection is being evaluated as a way to accelerate and increase oil recovery, through an improvement of the gravity drainage, main producing mechanism in this reservoir, and by pressure maintenance purposes, Arevalo-V, et al 1996 [13]. During the gas injection process, the injected gas composition is changed due to the vaporizing gas drive (VGD) mechanism, in which gas is enriched with intermediate molecular weight hydrocarbons from reservoir oil Yonebayashi et al, 2009 [14]. Recent studies indicate that gas injection of the water-invaded portion of the reservoir should recover additional oil.

LCSF Basic Data

LCSF fluid and rock properties were determined by laboratory experiments performed on samples of actual reservoir fluids. Table 1 shows the LCSF data.

Table 1: LCSF Data

Formation Producing	Cretaceous Limestone
Reservoir Temperature at Datum	180 deg F
Current Reservoir Pressure	2278 psig
Water Salinity	40474.59 ppg
Saturation Pressure	1100-1510 PSI
Differential Solution GOR	355 SCF/STB
F.V.F. at Original Pressure	1.245 RB/STB
API Gravity at 60 deg F	37 API
Density	43.0735 lb/ft^3
Viscosity	0.75 cp

Oil Compressibility	9×10^{-6}
Water Compressibility	3.30×10^{-6}

Fig. 1 shows the effective permeability to gas and effective permeability to oil for a given gas saturation, with the oil being considered the wetting phase. Fig. 2 shows the effective permeability to water and effective permeability to oil for a given water saturation with the water being considered the wetting phase.

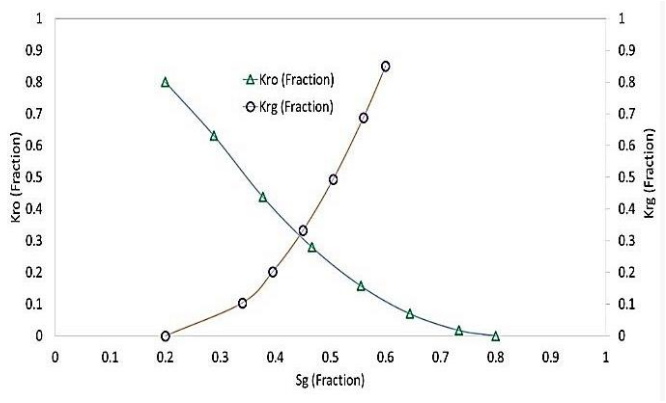

Fig. 1: Oil-Gas Systems

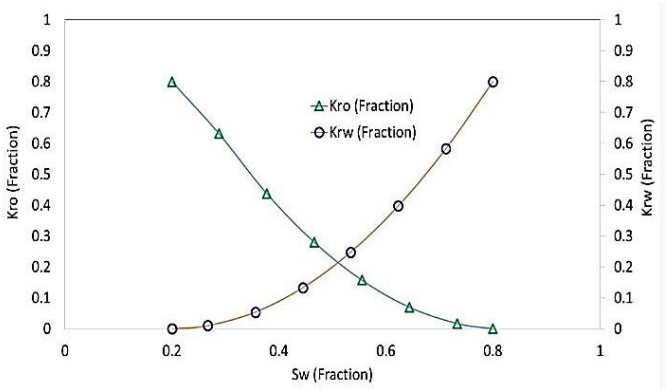

Fig. 2: Oil-Water Systems

LCSF Data Analysis

LCSF Fluid Data Analysis

This section will focus on the PVT analysis and production simulation of LCSF estimation by using MBAL software. The gas-oil ratio (GOR) is the ratio of the volume of gas ("scf") that comes out of solution to the volume of oil under standard conditions. When the reservoir pressure also decreases, the GOR decreases because the gas is liberated from the oil, as shown in Fig. 3.

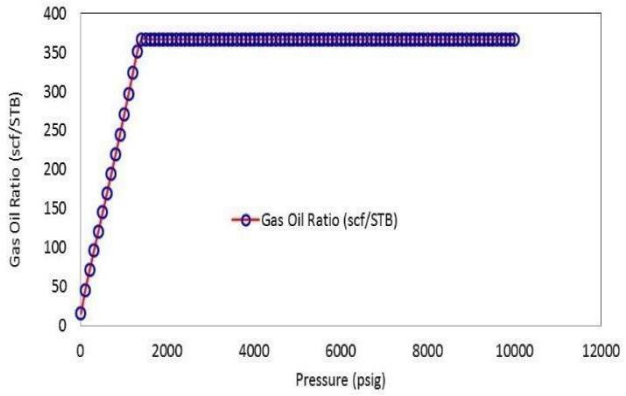

Fig. 3: LCSF Gas-Oil Ratio

Fig. 4 shows the oil, gas, and water viscosity vs pressure. Oil viscosity increases with a decrease in the pressure under saturated conditions due to the release of dissolved gas below the bubble point. For most liquids, viscosity increases with increasing pressure because the amount of free volume in the internal structure decreases due to compression. Consequently, the molecules can move less freely, and the internal friction forces increase.

Fig. 5 shows the oil, gas, and water formation volume factor. The figure shows that the formation volume factor is inversely proportional to pressure. This makes sense because as reservoir pressure declines, the gas will expand to occupy more volume in the reservoir. As we can see, Bg increases as reservoir pressure decreases. The water formation volume factor represents the change in volume of the brine as it is transported from the reservoir conditions to surface conditions. This shows that the oil formation volume factor increases with a reduction in pressure until the oil reaches the bubble-point pressure. The volume increase at pressures above the bubble point is due to the expansion of oil (with its dissolved gas). Below the bubble point, and with the continued reduction in pressure, the oil formation volume factor is reduced primarily due to mass loss with the additional release of dissolved gas.

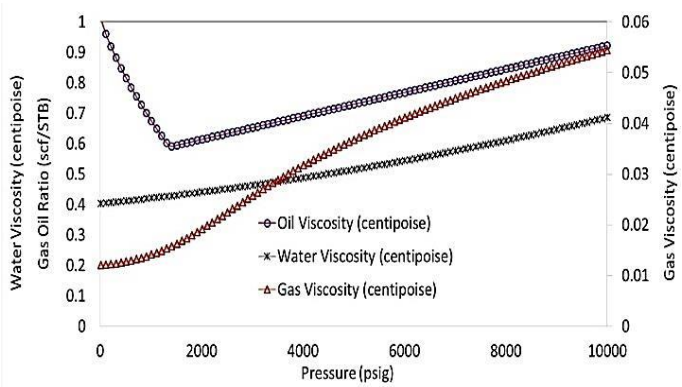

Fig. 4: LCSF Oil, Gas, and Water Viscosity

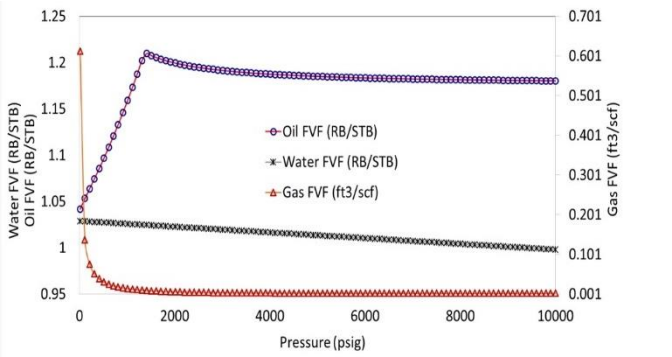

Fig. 5: LCSF Oil, Gas, and Water FVF

Fig. 6 shows the oil, gas, and water density. The oil density decreases with depletion of pressure until it reaches a minimum value at the bubble point. Gas density is a function of the pressure and temperature conditions for the gas. Due to its high compressibility, gas can change its volume significantly with changes in pressure. Understanding the compressibility of formation water is also important to understanding the volumes of oil, gas, and water in reservoir rock. It is the change in water volume per unit water volume per psi change in pressure.

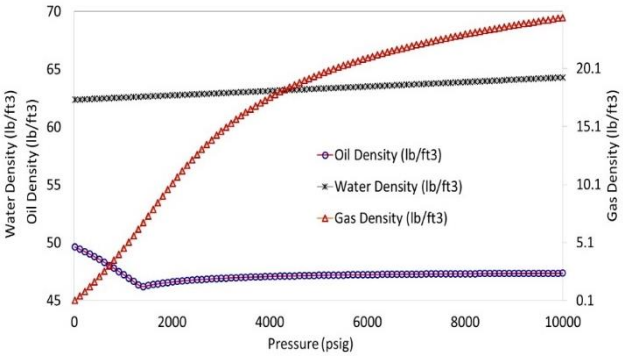

Fig. 6: LCSF Oil, Gas, and Water Density

LCSF Reservoir Potential Analysis and Depletion Analysis

This section will focus on the driving mechanism analysis and production simulation of LCSF estimation by using MBAL software. Fig. 7 shows the reservoir pressure history and simulation vs. time for an aquiver volume of 5177 mmft 3. The history reservoir pressure curve matches the stimulation curve, which gives a good allusion of the input data that have been entered into the model. By running the simulator with historical production and comparing it with the actual reservoir performance, the reservoir pressure is matched when the reservoir aquifer volume has been adjusted to 5177 mmft 3.

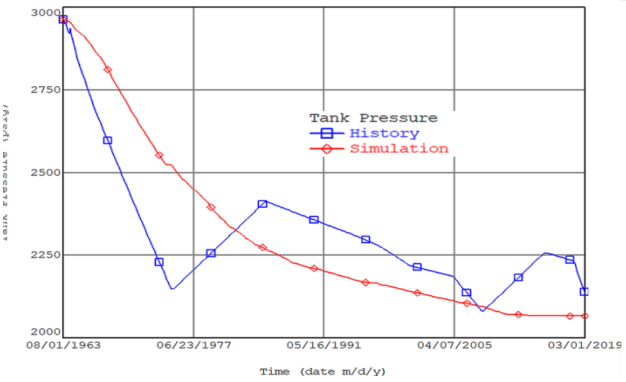

Fig. 7: LCSF Plotting Simulation Results

Fig. 8 shows the comparative contributions of the main source of energy in the reservoir and aquifer system vs time. From the below Fig., the drive mechanism for this reservoir consists of the following:

1. Fluid expansion ranges from 40 to 45%
2. Pore volume compressibility ranges between 45% and 55%.
3. Water Influx ranges between 5 and 15%

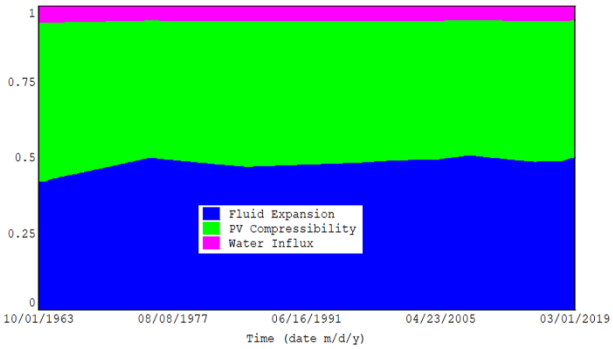

Fig. 8: LCSF Energy Plot

Field Liquid Potential Production Rate Analysis

Fig. 9 expresses the relation between the field oil, gas, and water potential production rates of oil vs time from 1963 to 2013. The time on the X-axis and the field oil, gas, and water production rates on the Y-axis. The graph shows that gas is produced per m-d-y. The graph shows that field initial gas production is approximately 12773,88 MSCF/day, field initial oil production is approximately 14494.125 STB/day, and field initial water production is approximately 0.36705735 STB/day.

Fig. 10 shows the field gas, oil, and water production total vs time. The Y-axis reflects the total production obtained from the gas, oil, and water wells, and the X-axis shows time. The total gas production is 1.3432202E+8 MSCF, the oil is 94873352 STB, and the total water production is 149287.33 STB.

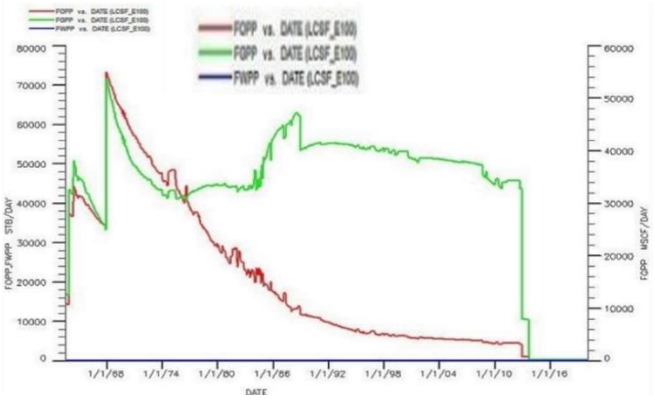

Fig. 9: FOPP, FGPP, and FWPP vs. Time

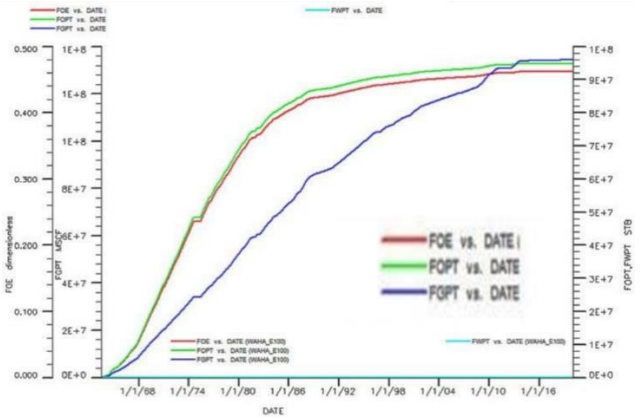

Fig. 10: FOE, FOPT, FGPT, and FWPT vs. Time

Graph 11 shows the field pressure, field water cut, and field oil efficiency vs time. The time is on the x-axis, and the field pressure, field water cut, and field oil efficiency are on the y-axis. The graph shows the effect of gas production on pressure with respect to time. The initial pressure is 3001 Psia, which decreases constantly with respect to time to 914 psia. The graph shows that the field oil efficiency is 0.46 and the field water cut is 0.00824.

LCSF Reservoir Simulation

LCSF Reservoir Geometry

Reservoir simulation is an area of reservoir engineering where computer models are used to predict the flow of fluids through porous media. We built reservoir models that include the petrophysical characteristics required to understand the behavior of the fluids over time.

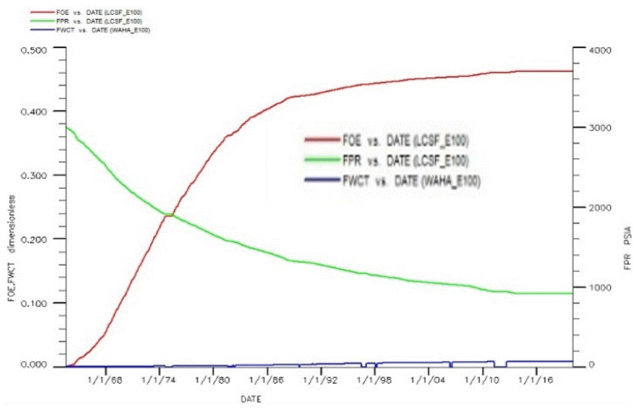

Fig. 11: FOE, FPR, and FWCT vs. Time

The simulator is calibrated using historic pressure and production data in a process referred to as history matching. Once the simulator has been successfully calibrated, it is used to predict future reservoir production under a series of potential scenarios, such as drilling new wells, injecting various fluids or stimulation. Fig. 12 shows the LCSF reservoir model and location map. The reservoir grid is made of 57 x 46 x 56 = 146832 cells.

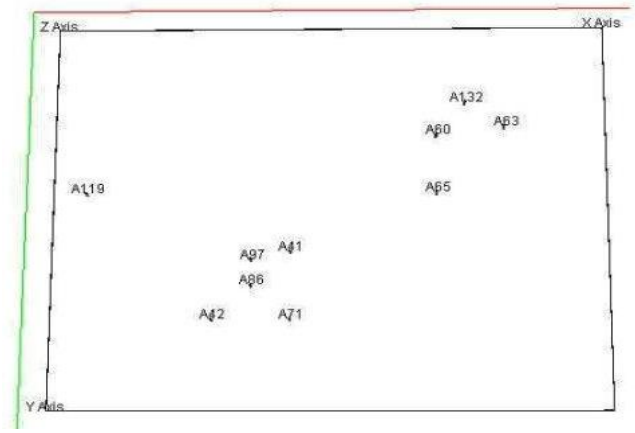

Fig. 12: LCSF Reservoir Model and Location Map

Fig. 13 demonstrates that the permeability variation of the first layer is altered between 0.62 and 536 mD, with an average permeability of approximately 268.31 mD.

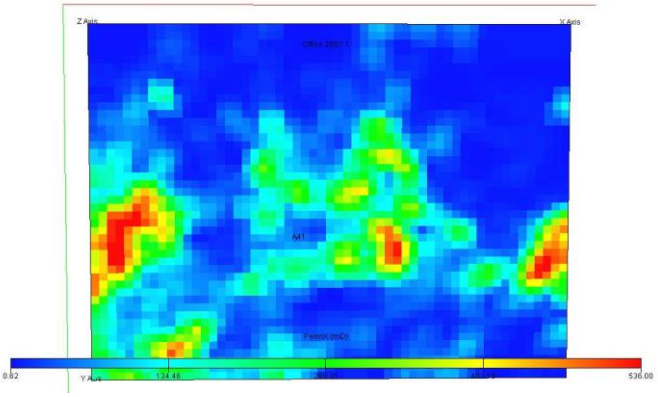

Fig. 13: LCSF Permeability Distribution in Layer 1

Fig. 14 demonstrates that the porosity variation of the first layer is altered between 0.061 and 0.348 with an average porosity of approximately 0.20

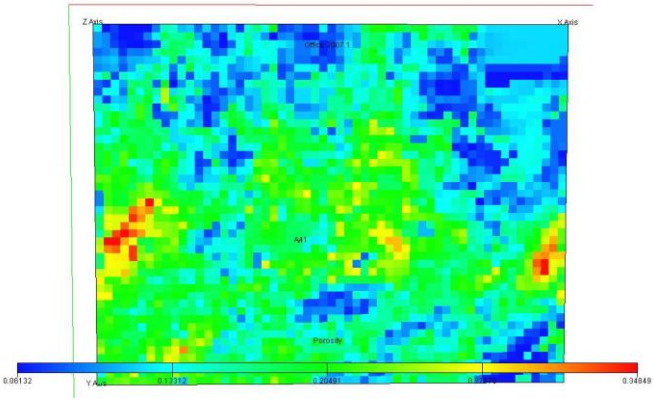

Fig. 14: LCSF Porosity Distribution in Layer 1

Fig. 15 demonstrates that the initial oil saturation variation of the first layer is altered between 0.67 and 0.82, with an average initial oil saturation of approximately 0.45

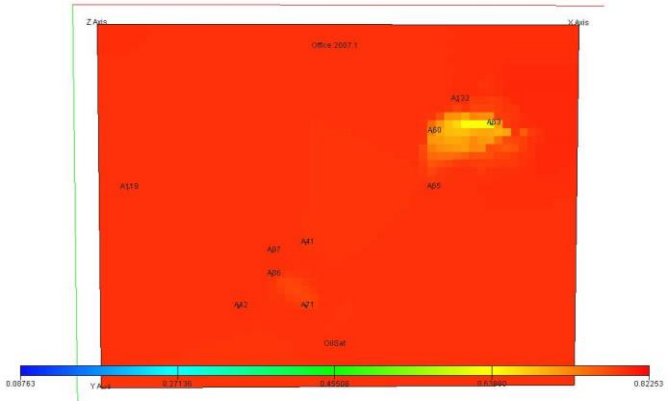

Fig. 15: LCSF Initial Oil Saturation in Layer 1

Fig. 16 demonstrates that the initial water saturation variation in the first layer is altered between 0.17 and 0.91, with an average initial water saturation of approximately 0.54

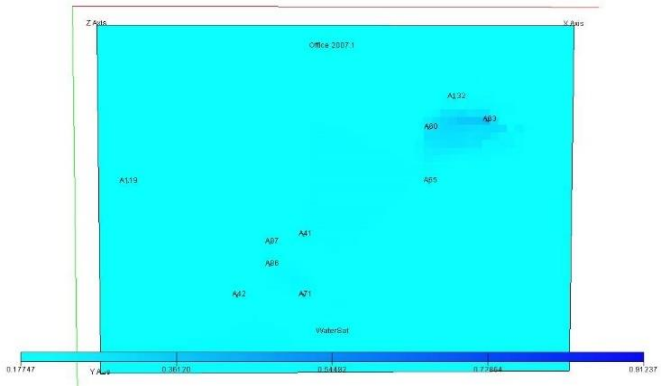

Fig. 16: LCSF Initial Water Saturation in Layer 1

Fig. 17 demonstrates that the initial pressure distribution of the first layer is altered between 2617 psi and 3450 psi with an average pressure of approximately 3038 psi.

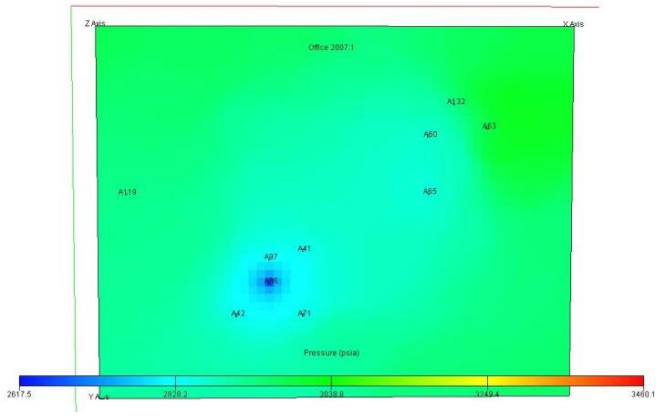

Fig. 17: LCSF Initial Pressure Distribution in Layer 1

LCSF History Matching

The act of adjusting a model of a reservoir until it closely reproduces the past behavior of a reservoir. The historical production and pressures are matched as closely as possible. Fig. 18 shows the production rate history matching results for well A60, and Fig. 19 shows the production rate history matching results for well A86.

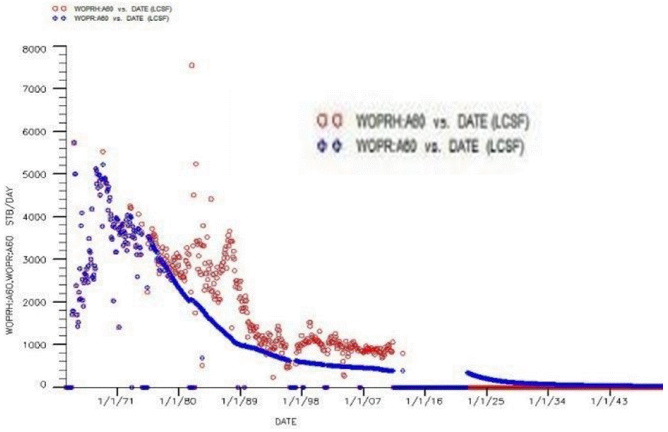

Fig. 18: Well, A60 Oil Production Rate History Matching results.

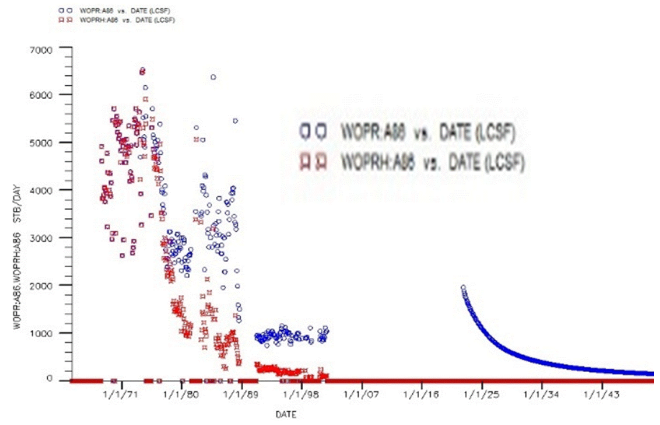

Fig. 19: Well, A86 Oil Production Rate History Matching results.

LCSF Prediction Without any Injection

This section will show the results of the LCSF prediction by natural reservoir energy, such as gas drive, water drive or gravity drainage, displacing hydrocarbons from the reservoir into the wellbore and up to the surface from 2013 to 2043. This scenario is called the Base Case. Fig. 20 shows the FOPP, FGPP, and FWPP vs. Time.

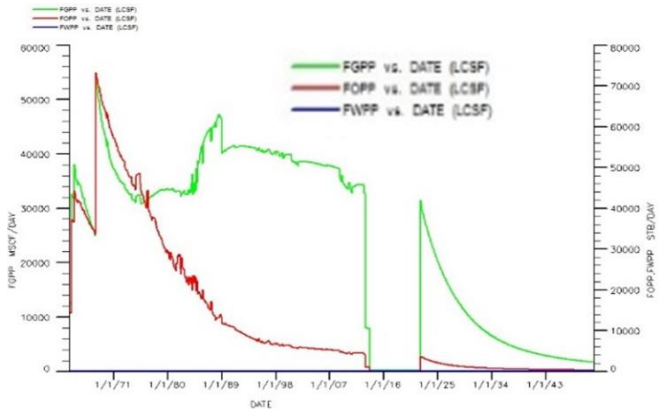

Fig. 20: FOPP, FGPP, and FWPP vs. Time (Base Case)

Fig. 21 shows the field gas, oil, and water production total vs time. The Y-axis reflects the total production we obtain from the gas, oil, and water wells, and the X-axis shows time. A total of 2.2081352E+8 MSCF of gas, 1.0449847E+8 STB of oil, and 297935.25 STB of water are produced.

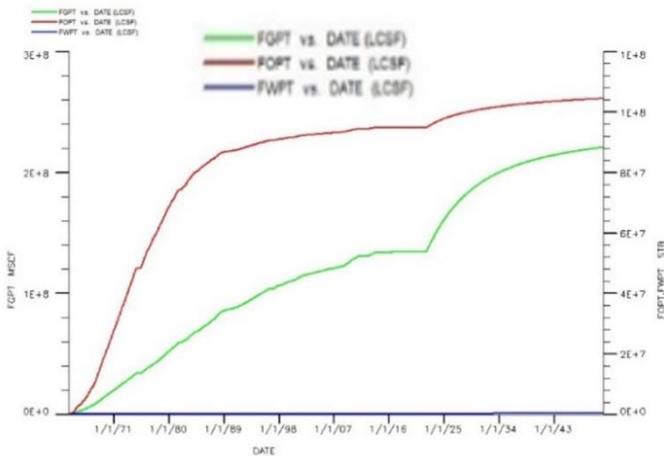

Fig. 21: FOPT, FGPT, and FWPT vs. Time (Base Case)

Graph 22 shows field pressure, field water cut, and field oil efficiency vs time. The time is on the x-axis, and the field pressure, field water cut, and field oil efficiency are on the y-axis. The graph shows that the pressure is increasing constantly with respect to time to 192.43611 psia. The graph shows that the field oil efficiency is 0.50884378 and the field water cut is 0.021935357.

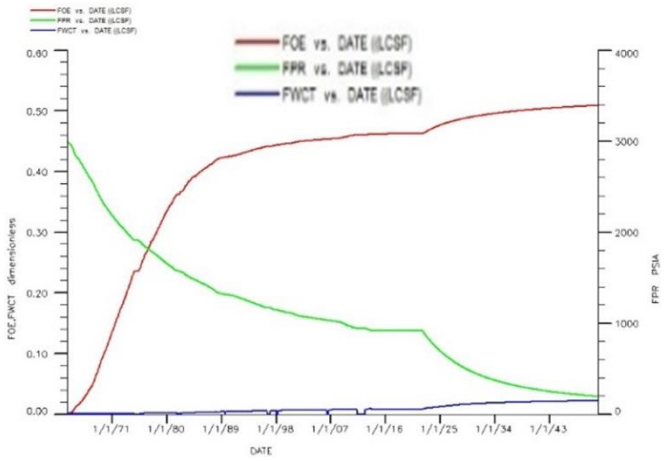

Fig. 22: FOE, FPR, and FWCT vs. Time (Base Case)

LCSF Secondary Recovery

Injector Well Location: Secondary recovery techniques involve supplementing the natural energy of a petroleum reservoir by the injection of fluids, normally water or gas. Normally, gas is injected into the gas cap, and water is injected into the production zone to sweep oil from the reservoir, as shown in Fig. 23 and Fig. 24.

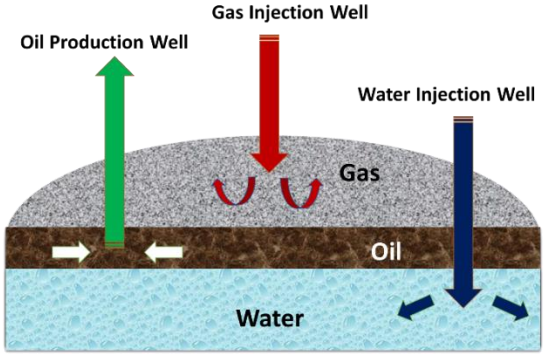

Fig. 23: Gas and Water Injection, Oil Well Production

Injector Well Rate: After we know which zone we will Inject; which wells will convert and how much the bottom hole pressure target for each Injector wells. Now, we start to inject water, but before that, we must estimate the best rate of water for each well injector. To estimate the best rate, we can inject. We will play with the rate of injection for each injector well, as shown in table 2 and figure 25.

Table 1: Injection Rate

Scenarios	Rate Injection Well	Total Gas Injection Well
	SCF/DAY	SCF/DAY
Scenario#1	**Base Case**	**0**
	250	750
	500	1500
	750	2250
	1000	3000
	1250	3750
	1500	4500
	1750	5250
	2000	6000
	2250	6750
	2500	7500
Scenario#2	5000	15000
	10000	30000
	15000	45000
	20000	60000
	25000	75000
	30000	90000
Scenario#3	50000	150000
	100000	300000
	150000	450000
	200000	600000
	250000	750000
	300000	900000
Scenario#4	500000	1500000
	1000000	3000000
	1500000	4500000
	2000000	6000000
	2500000	7500000
	3000000	9000000

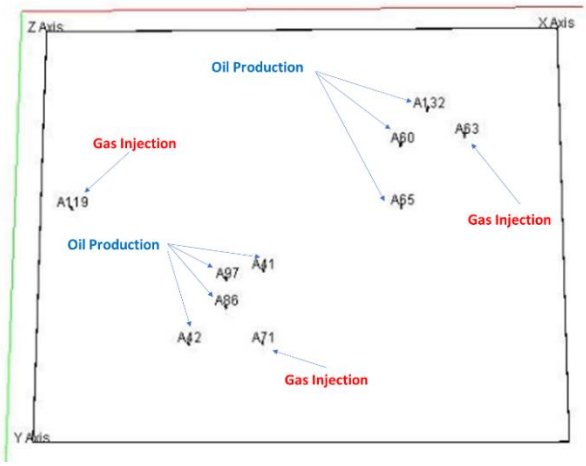

Fig. 24: LCSF Oil Production and Injection Well Location

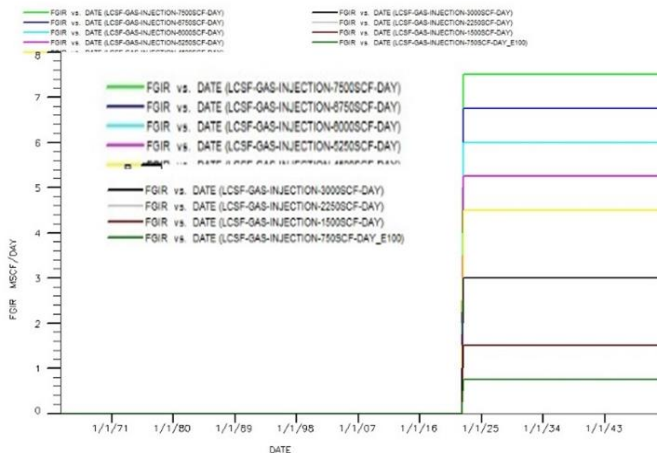

Fig. 25: Field Gas Injection Rate Scenario#1

Fig. 26 and Table 3 express the relation between the field gas potential production rate vs time from 2013 to 2043 for Scenario#1. The time on the X-axis and the field gas production rate on the Y-axis. The graph shows that gas is produced per m-d-y.

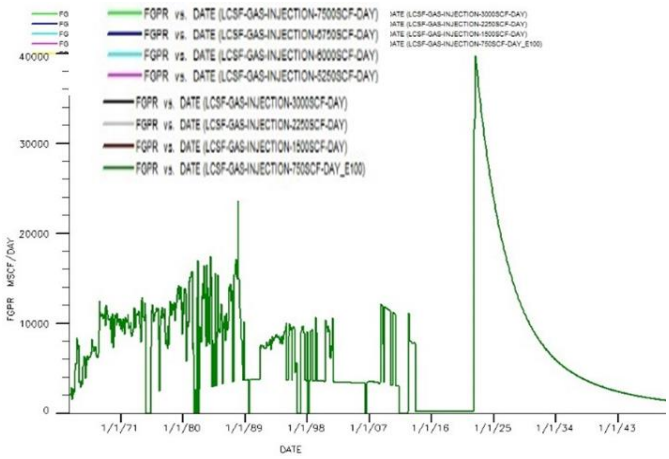

Fig. 26: Field Gas Production Rate Scenario#1

Fig. 27 and Table 3 express the relation between the field oil potential production rate vs time from 2013 to 2043 for Scenario#1. The time on the X-axis and the field oil production rate on the Y-axis.

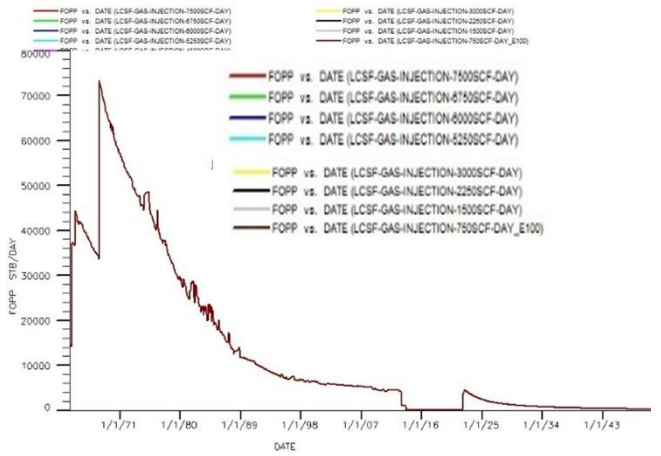

Fig. 27: Field Oil Production Rate Scenario#1

Graph 28 shows field pressure vs time. The time is on the x-axis, and the field pressure is on the y-axis. The graph shows that the pressure is increasing constantly with respect to time.

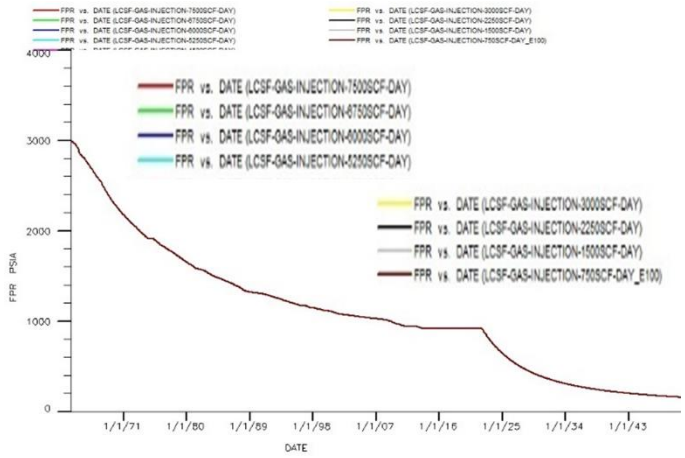

Fig. 28: Field Pressure Scenario#1

Graph 29 shows the field water cut vs time. The time is on the x-axis, and the field water cut is on the y-axis. The graph shows that the field water cut is increasing constantly with respect to time.

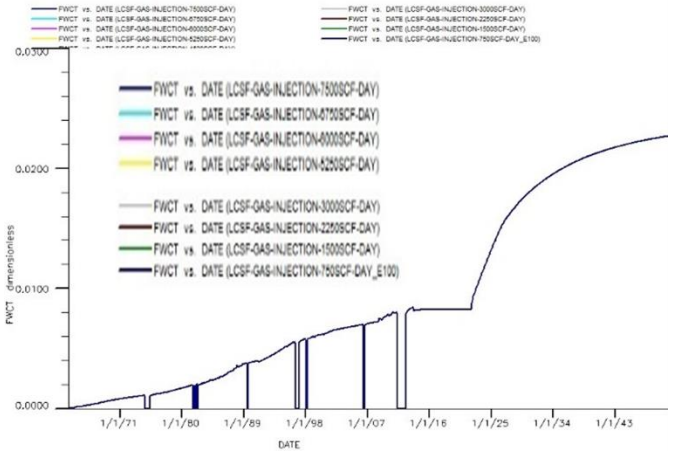

Fig. 29: Field Water Cut Scenario#1

Graph 30 shows the field oil efficiency vs time. The time is on the x-axis, and the field oil efficiency is on the y-axis. The graph shows that the field oil efficiency is increasing constantly with respect to time.

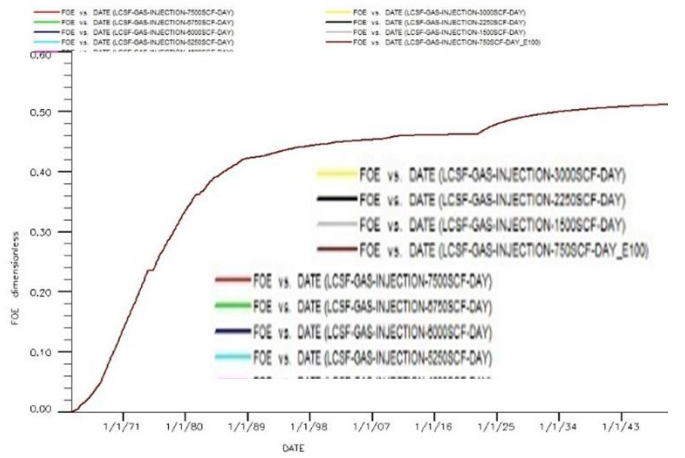

Fig. 30: FOE Scenario#1

Graph 31 shows the field oil production total vs time. The time is on the x-axis, and the field oil production total is on the y-axis. The graph shows that the field oil production total is increasing constantly with respect to time.

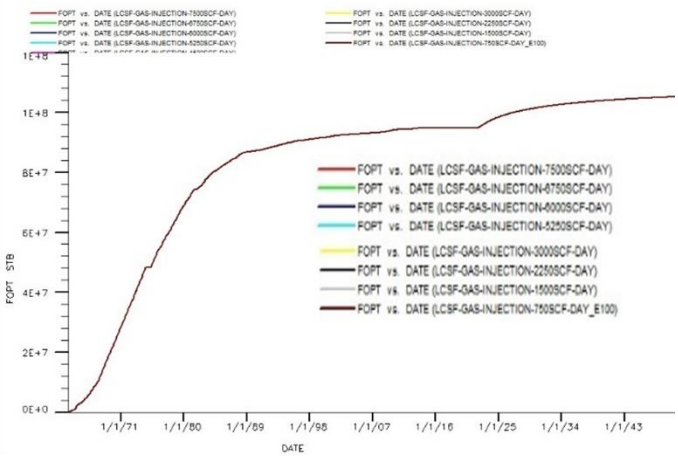

Fig. 31: Field Oil Production Total Scenario#1

Graph 32 shows the field gas injection total vs time. The time is on the x-axis, and the field gas injection total is on the y-axis.

Fig. 33 demonstrates the gas saturation distribution at the end of scenario #1 of the first layer. It is altered between 0.12 and 0.71, with an average gas saturation distribution of approximately 0.41.

Fig. 34 demonstrates the oil saturation distribution at the end of scenario #2 of the first layer. It is altered between 0.06 and 0.76, with an average oil saturation distribution of approximately 0.414.

Fig. 35 demonstrates the water saturation distribution at the end of scenario #3 of the first layer. It is altered between 0.12 and 0.1213, with an average water saturation distribution of approximately 0.12007.

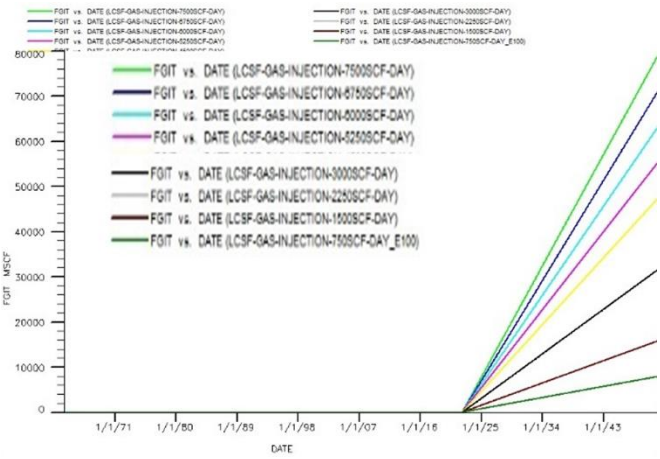

Fig. 32: Field Gas Injection Total Scenario#1

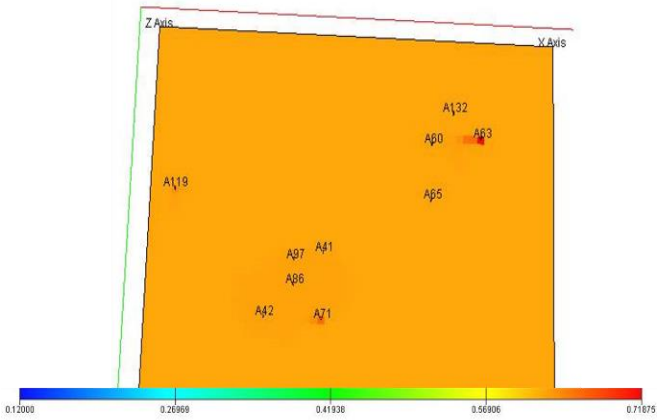

Fig. 33: Gas saturation distribution at the end of Scenario #1

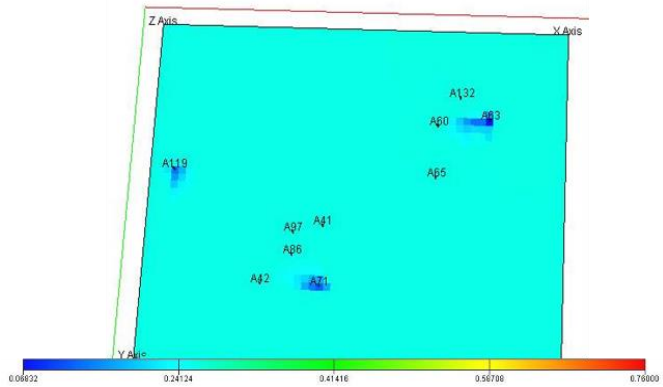

Fig. 34: Oil Saturation Distribution at the end of Scenario #2

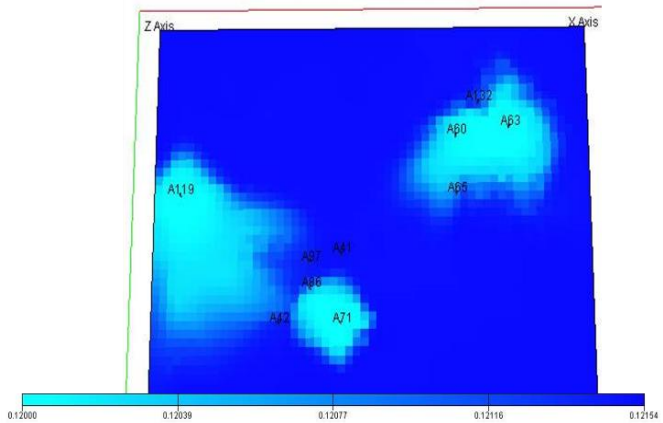

Fig. 35: Water Saturation Distribution at the end of Scenario #3

Scenarios Comparison

Fig. 36 expresses the relation between the field oil, gas, and water production total of oil vs different rates for all the scenarios. The time on the X-axis and the field oil, gas, and water production total on the Y-axis. The oil production total graph shows the effect of gas injection rates on oil production. The injection rate shows good performance overall, as indicated by the cumulative oil production.

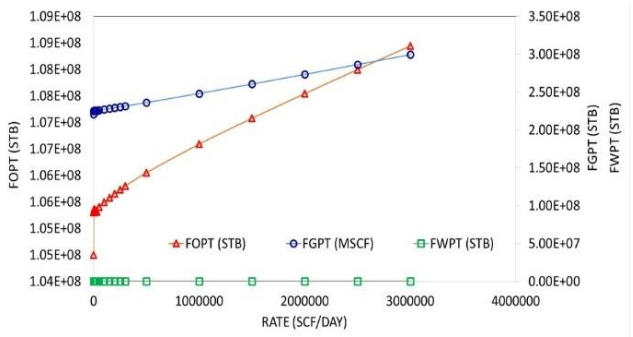

Fig. 36: FOPT, FGPT, and FWPT Scenario Comparison

Graph 37 shows field pressure vs. different rates. The different rates are on the x-axis, and the field pressure is on the y-axis. The graph shows the effect of gas injection on pressure. Additionally, in graph 37 shows field gas injection total vs different rates. The different rates are on the x-axis, and the field gas injection total is on the y-axis.

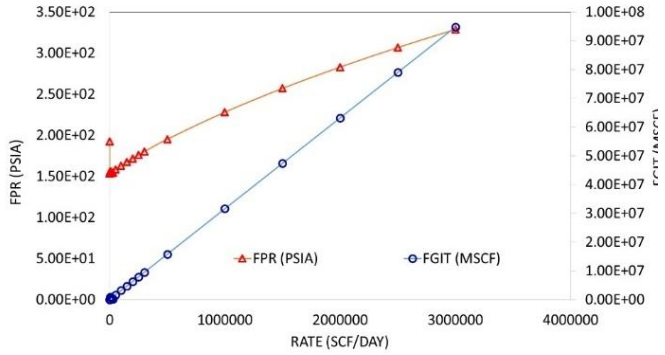

Fig. 37: FPR and FGIT Scenario Comparison

Graph 38 shows the field water cut vs different rates. The different rates are on the x-axis, and the field water cut is on the y-axis. The graph shows the effect of gas injection on the water cut. Additionally, in graph 38 shows field oil efficiency vs different rates. The different rates are on the x-axis, and the field oil efficiency is on the y-axis.

Conclusion and Recommendation

As a comprehensive reservoir study for the LCSF plane of development, this study covered analyses and evaluation. In this project, we obtain the following conclusions:

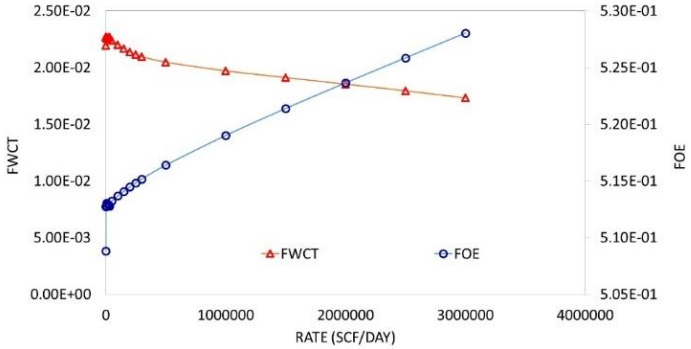

Fig. 38: FOE and FWCT Scenario Comparison

1. The main reservoir driving force in the LCSF is fluid expansion. First, fluid expansion ranges from 40 to 45%. Second, pore volume compressibility ranges between 45 and 55%. Water Influx ranges between 5 and 15%.
2. The reservoir in the LCSF is a reservoir with fluid expansion. In developing this reservoir, the main driving mechanism to control production is gas drive. Gas injection is taken into consideration in the development plan to give a higher FOPT and FOE.
3. The location of production and injection wells influences the oil production rate and recoverable reserve. Time management is also one of the most influential factors in producing and developing oil in LCSF. The right time to inject water and gas is very important so that the reservoir pressure can be maintained.
4. The gas injection scenario has a good plateau bpd that lasts approximately 3 years and then starts to decrease. The cumulative oil production is 108442340 STB barrels of oil with a recovery factor of approximately 0.52805, and the final reservoir pressure is maintained at 328.76 psi.

References

[1] Naser, M. A., Erhayem, M., Hegaig, A., Abdullah, H. J., Amer, M. Y., & Mohamed, A. A. (2018). Comparative Study of Using Sea-Water for Enhanced Oil Recovery in Carbonate and Sandstone Reservoirs: Effects of Temperature and Aging Time on Oil Recovery. Journal of Earth Energy Engineering, 7(2), 1-13. https://doi.org/10.25299/jeee.2018.vol7(2).2126

[2] Mohammed Samba, Yiqiang Li, Madi Abdullah Naser, Mahmoud O Elsharafi. Comparison of Different Gases Injection Techniques for Better Oil Productivity; Journal of Petroleum and Geothermal Technology, https://doi.org/10.31315/jpgt.v2i1.4009

[3] Dong, Cuiyu, and B. Todd Hoffman. "Modelling Gas Injection into Shale Oil Reservoirs in the Sanish Field, North Dakota." Paper presented at the SPE/AAPG/SEG Unconventional Resources Technology Conference, Denver, Colorado, USA, August 2013. doi: https://doi.org/10.1190/urtec2013-185

[4] Baojun, Feng, Xingjia, Du, and Yu Cai. "Pilot Test of Water Alternating Gas Injection in Heterogeneous Thick Reservoir of Positive Rhythm Sedimentation of Daqing Oil Field." SPE Advanced Technology Series 5 (1997): 41–48. doi: https://doi.org/10.2118/30842-PA

[5] Hedjazi, A.K. "Gas Injection In City Of Inglewood Pool Inglewood Oil Field - California." Paper presented at the SPE California Regional Meeting, Los Angeles, California, October 1967. doi: https://doi.org/10.2118/1990-MS

[6] Vowel, W.R.. "Gas Injection in Eastern Venezuela Field Increases Oil Recovery." J Pet Technol 10 (1958): 31–33. doi: https://doi.org/10.2118/1103-G

[7] Tang, Xueqing , Wang, Ruifeng , and Hui Zhang. "Innovative Field-Scale Application of Injecting Condensate Gas and Recycling Gas into Medium Oil Pool: Case Study in Sudan." Paper presented at the SPE Enhanced Oil Recovery Conference, Kuala Lumpur, Malaysia, July 2013. doi: https://doi.org/10.2118/165289-MS

[8] Gong, Houjian, Zhang, Huan, Lv, Wei, Xu, Long, Li, Zijin, and Mingzhe Dong. "Effects of Kerogen on the Flow and EOR Performance of Oil in Shale Cores during CO2 Flooding Process Investigated by NMR Technology." SPE J. (2022;): doi: https://doi.org/10.2118/209581-PA

[9] Ibe, Alonge, Olafuyi, Olalekan, Anim, John, Etim, Christopher, Ameachi, Ntietemi, Olusola, Bukola, Kpone-Tonwe, Hannah, and Patrick Obah. "Numerical Simulation of Gas Injection for Condensate Revaporization in Gas Condensate Reservoirs. A Field Case Study." Paper presented at the SPE Nigeria Annual

International Conference and Exhibition, Lagos, Nigeria, August 2022. doi: https://doi.org/10.2118/212042-MS

[10] Ariffin, Mohd Hafizi, Guillory, Ryan, Low, Bee Chan, and Fairus Azwardy Salleh. "Striving Towards Zero Gas Emission." Paper presented at the Offshore Technology Conference Asia, Virtual and Kuala Lumpur, Malaysia, March 2022. doi: https://doi.org/10.4043/31392-MS

[11] Rotelli, F., Blunt, M. J., De Simoni, Michela, Dovera, L., Rotondi, M., and A. Lamberti. "CO2 Injection in Carbonate Reservoirs: Combining EOR and CO2 Storage." Paper presented at the Offshore Mediterranean Conference and Exhibition, Ravenna, Italy, March 2017.

[12] Jethwa, D.J., Rothkopf, B.W., and C.I. Paulson. "Successful Miscible Gas Injection in a Mature U.K. North Sea Field." Paper presented at the SPE Annual Technical Conference and Exhibition, Dallas, Texas, October 2000. doi: https://doi.org/10.2118/62990-MS

[13] Arevalo-V., J.A., Samaniego-V., F., Lopez-C., F.F, and E. Urquieta-S. "On the Exploitation Conditions of the Akal Reservoir Considering Gas Cap Nitrogen Injection." Paper presented at the International Petroleum Conference and Exhibition of Mexico, Villahermosa, Mexico, March 1996. doi: https://doi.org/10.2118/35319-MS

[14] Yonebayashi, Hideharu, Al Mutairi, Ali Mohamed, Al-Habshi, Ali Mohamed, and Daisuke Urasaki. "Dynamic Asphaltene Behavior for Gas Injection Risk Analysis." Paper presented at the International Petroleum Technology Conference, Doha, Qatar, December 2009. doi: https://doi.org/10.2523/IPTC-13266-MS

Notation	
BOPD	Barrel Oil Production Per Day
DX	Dimensions of a Grid Cell in X Direction
DZ	Dimensions of a Grid Cell in Z Direction
DY	Dimensions of a Grid Cell in Y Direction
OOIP	Originally Oil In Place
EOR	Recovery Factor
FOPT	Field Oil Production Total
FOPR	Field Oil Production Rate
FPR	Field Reservoir Pressure
FGOR	Field Gas-Oil Ratio
FWCT	Field Water Cut

SCENARIOS COMPARISON:

RATE	TOTAL	FGPT	FOE	FOPT	FPR	FWCT	FWPT	FGIT
SCF/DAY	SCF/DAY	(MSCF)		(STB)	(PSIA)		(STB)	(MSCF)
0	0	220813520	0.50884	104498470	192.44	0.02194	297935	0
250	750	225242860	0.51276	105303620	153.41	0.02271	317008	7897.5
500	1500	225247940	0.51277	105304100	153.44	0.02271	317016	15795
750	2250	225247940	0.51277	105304100	153.44	0.02271	317016	15795
1000	3000	225258130	0.51277	105305090	153.49	0.02271	317032	31590
1250	3750	225263200	0.51277	105305580	153.51	0.02271	317040	39487.5
1500	4500	225268270	0.51278	105306070	153.54	0.02271	317048	47385
1750	5250	225273340	0.51278	105306570	153.56	0.02270	317056	55282.5
2000	6000	225278430	0.51278	105307060	153.58	0.02270	317063	63180
2250	6750	225283520	0.51278	105307550	153.61	0.02270	317071	71077.5
2500	7500	225288610	0.51279	105308040	153.63	0.02270	317079	78975
5000	15000	225851940	0.51305	105361980	156.31	0.02256	317885	947700
10000	30000	225749040	0.51300	105352270	155.82	0.02259	317748	789750
15000	45000	225646340	0.51295	105342510	155.34	0.02262	317606	631800
20000	60000	225543820	0.51291	105332690	154.86	0.02265	317460	473850
25000	75000	225441580	0.51286	105322830	154.37	0.02267	317311	315900
30000	90000	225339540	0.51281	105312980	153.88	0.02269	317157	157950
50000	150000	226265700	0.51323	105400200	158.21	0.02242	318397	1579500
100000	300000	227314620	0.51368	105491220	162.86	0.02204	319477	3159000
150000	450000	228382290	0.51409	105576090	167.34	0.02168	320365	4738500
200000	600000	229467180	0.51448	105655420	171.67	0.02139	321138	6318000
250000	750000	230568220	0.51484	105729660	175.86	0.02116	321832	7897500
300000	900000	231682270	0.51518	105799760	179.94	0.02098	322478	9477000
500000	1500000	236262700	0.51640	106050560	195.16	0.02049	324773	15795000
1000000	3000000	248231090	0.51902	106589440	228.11	0.01972	329892	31590000
1500000	4500000	260650080	0.52140	107076730	256.98	0.01913	334593	47385000
2000000	6000000	273391680	0.52366	107542110	282.95	0.01855	339018	63180000
2500000	7500000	286382620	0.52587	107996170	306.66	0.01796	343176	78975000
3000000	9000000	299563360	0.52805	108442340	328.76	0.01733	347008	94770000